Perfect conformal invisible device with feasible refractive indexes

Lin Xu, Huanyang Chen, Tomáš Tyc, Yangbo Xie, and Steven A. Cummer

Phys. Rev. B **93**, 041406 — Published 6 January 2016

DOI: 10.1103/PhysRevB.93.041406

A perfect conformal invisible device with feasible refractive indexes

Lin Xu and Huanyang Chen*
College of Physics, Optoelectronics and Energy & Collaborative Innovation Center of Suzhou Nano Science and Technology, Soochow University, No.1 Shizi Street, Suzhou 215006, China
Tomas Tyc
Department of Theoretical Physics and Astrophysics, Masaryk University, Kotlarska 2, 61137 Brno, Czech Republic
Yangbo Xie and Steven A. Cummer
Department of Electrical and Computer Engineering, Duke University, Durham, North Carolina 27708, USA.

Optical conformal mapping has been used to construct several isotropic devices with novel functionalities. In particular, a conformal cloak could confer omnidirectional invisibility. However, the maximum values of the refractive indexes needed for current designs are too large to implement, even in microwave experiments. Furthermore, most devices designed so far have had imperfect impedance matching, and therefore incomplete invisibility functionalities. Here we describe a perfect conformal invisible device with full impedance matching everywhere – the first description of such a device, to the best of our knowledge. The maximum value of refractive index required by our device is just about five, which is feasible for microwave and THz experiments using current metamaterial techniques. To construct the device, we use a logarithmic conformal mapping and a Mikaelian lens. Our results should enable a conformal invisible device with almost perfect invisibility to be made soon.

I. INTRODUCTION

Transformation optics (TO) has shown great versatility for controlling light propagation since the two pioneering papers on invisibility were first published [1,2]. Numerous functions using TO have now been proposed, such as invisible cloaking [1-4], carpet cloaking [5,6], field concentration [7,8], and rotation [9,10]. Such developments have been described in several recent reviews [11-14]. Besides optical waves, this approach has been also extended to manipulation of other waves, such as acoustic waves [15-17].

As a special method in two dimensions, conformal transformation optics (CTO) [1,18] gives us a simpler routine to control light or waves with only isotropic refractive index distributions, avoiding complicated electromagnetic tensor analysis. Many functionalities of conformal devices have been proposed, such as invisible cloaking [1,19,20], light bending [21,22] and imaging [23]. But as far as we know, only two conformal devices using isotropic materials have been reported experimentally. One [24] generates collimated light rays by Möbius mapping; the other [25] achieves one-dimensional cloaking by Zhukowski mapping. What hinders the development of CTO is the difficulty of optimizing the range of refractive-index variation, and especially reducing

* chy@suda.edu.cn

the maximum values required. In an earlier design for conformal invisible device [1], the range of the designed refractive index is from 0 to about 36, which is a major challenge for electromagnetic waves. Following the same conformal mapping, two "kissing" mirrored Maxwell's fisheye lenses have been introduced to reduce the maximum of refractive index to about 13 [18]. Recently, it was reported that the maximum refractive index can be further reduced to 9.8 by using dual logarithm conformal mapping with a linear term [19]. However, these values are still hard to attain experimentally. Apart from these, other kinds of isotropic invisible devices also exist, such as invisible cylinders or invisible spheres [26,27]. However, there are infinitely large values of refractive indexes in such devices, hence nearly impossible to attain.

Here we design a new conformal invisible device by applying a conformal logarithmic mapping with a linear term [19,21] to a Mikaelian lens [28,29] - the first time this optical device has been used in invisibility designs. Surprisingly we find that this design offers perfect invisibility, thanks to impedance matching everywhere, while requiring a maximum refractive index of just 5.21. Numerical simulation confirms our theoretical result. We also find that a perfect electric conductor (PEC) can be almost perfectly hidden by this device from any incident direction.

II.Results

A. Conformal logarithmic mapping with a linear term.

In mathematics, a conformal mapping [17, 30] in two dimensions is usually described by a complex analytic function (in the form of $w=f(z)$), which only depends on z but not its complex conjugate z^*. In this letter, we focus on a special kind of conformal mapping: conformal logarithmic mapping with a linear term [19], which is written as

$$w(z)=z+\alpha[\log(z-\beta)-\log(z+\beta)], \qquad (1)$$

where α and β are two free real variables. This mapping has one linear term (z) and two dual logarithmic terms ($\log(z-\beta)$ and $\log(z+\beta)$), and possesses two singularities ($-\beta+0*\mathrm{i}$ and $\beta+0*\mathrm{i}$). It is not hard to see that w approaches z for $z\to\infty$.

For some values of w_0 in the domain of this mapping, there are two different corresponding values z_1 and z_2. The one-to-one mapping between the domain (z-space, physical space) and range (w-space, virtual space) is shown in Fig. 1: the physical space is a whole complex plane (denoted by $z=x+yi$ in Fig. 1(c)), while the corresponding virtual space is constructed as a Riemann surface [31] (described by $w=u+vi$ in Fig. 1(a)). The Riemann surface consists of two Riemann sheets: the lower sheet (black mesh on blue) is a whole complex plane, while the upper sheet (green mesh on green) is a ribbon-like complex plane, owing to the periodicity of logarithmic terms in the conformal mapping. Both sheets are connected with a branch cut (shown in yellow). Thick green lines at the boundaries along the u direction indicate that the upper sheet is finite in the v direction. If we roll the upper sheet along the u direction and glue the two boundaries, we obtain a cylindrical surface. So we can intuitively re-plot this virtual space with the equivalent diagram shown in Fig. 1(b). The ends of cylindrical surface are mapped from two singularities of physical space. In Fig. 1(a), the width of the upper sheet is $d=2\alpha\pi$, and

the length of the branch cut is no larger than d, which depends on the parameters α and β. The middle point of the branch cut is the origin of both Riemann sheets. The whole structure in virtual space comes from physical space by the conformal mapping expressed in Eq. (1). The branch cut is mapped from circle-like curve (also in yellow). Every point of the branch cut corresponds to two points of this circle-like curve: in other words, one can imagine the branch cut being blown up to circle-like curve. In the equivalent diagram Fig. 1(b), the perimeter of the cylindrical surface is the same as the width of the upper sheet in Fig. 1(a). Here the branch cut changes into part of a circle.

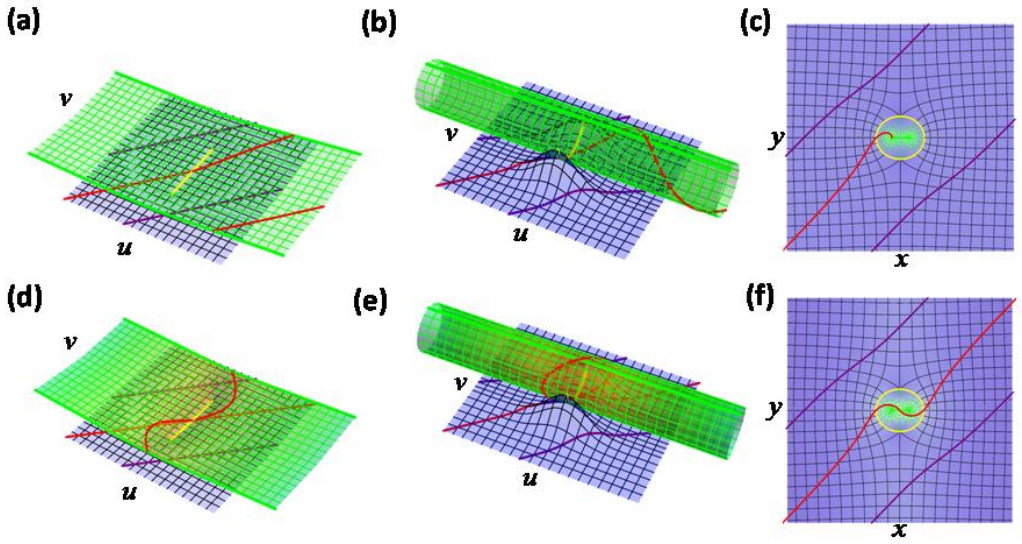

FIG. 1. (a) Virtual space of conformal logarithmic mapping. (b) The equivalent diagram of virtual space of conformal logarithmic mapping. (c) Physical space of conformal logarithmic mapping. (d) Virtual space of conformal invisibility. (e) The equivalent diagram of virtual space of conformal invisibility. (f) Physical space of conformal invisibility.

In conformal transformation optics [17], once we know the structure of virtual space and physical space of the conformal mapping expressed in Eq. (1), it is easy to deduce the propagation of light in both spaces. Suppose that the refractive index distributions of virtual space and physical space are n_w and n_z, respectively. The conformal mapping preserves the optical path between virtual space and physical space by [1]

$$n_z = n_w |\mathrm{dw}/\mathrm{dz}|, \qquad (2)$$

which implies that the materials are isotropic in physical space. Suppose for simplicity that n_w=1 at every point in virtual space, which means that light rays propagate along straight lines in both Riemann sheets. In Fig. 1(a) , one light ray (in red) propagates along a straight line in the lower sheet and hits the branch cut. Then it enters onto the upper sheet. Once it meets a boundary (one of the thick green lines) of the upper sheet, it will appear at another boundary (another

thick green line) and gradually goes to infinity. As shown in the equivalent diagram Fig. 1(b), this light ray (in red) has a helical trajectory on the cylindrical surface. In physical space shown in Fig. 1(c), this becomes a spiral curve (in red), which tends to one of singularities of the conformal mapping. As for the two parallel light rays shown in purple in Fig. 1(a), they will not meet the branch cut and will simply propagate in straight lines. The equivalent rays are shown in Fig. 1(b), and their trajectories under this conformal mapping are shown as purple curves in Fig. 1(c), which are geodesics of physical space.

B. Mikaelian lens

The conformal mapping determines the relationship between virtual space and physical space, so we can know how light rays travel in physical space by working out their behavior in virtual space. Virtual space is usually constructed as a Riemann surface, which is locally flat ($n_w = 1$). Once we introduce a refractive index profile into this virtual space, we can manipulate light rays at will. Here we introduce a special refractive index profile: the Mikaelian lens [28,29].

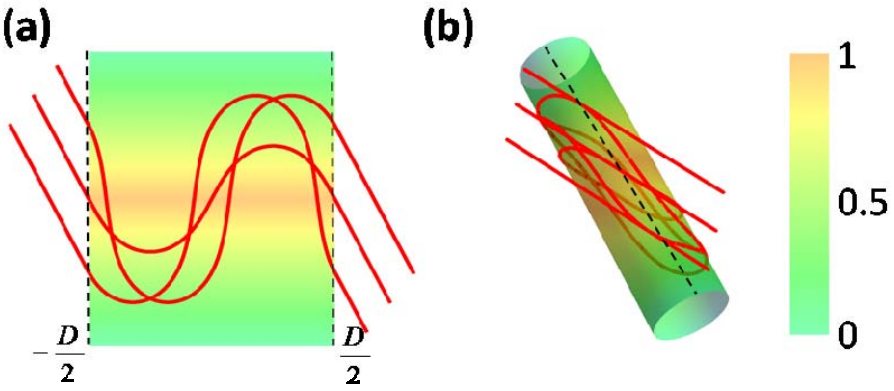

FIG. 2. (a) Two dimensional truncated Mikaelian lens with a single period. For parallel light rays (in red) , they propagate along a sine-like curve and then leave the lens at the same height in the original direction. (b) When we roll truncated Mikaelian lens into a cylindrical surface, trajectories of corresponding light rays are all closed.

The Mikaelian lens was first described as a self-focusing cylindrical medium with axial symmetry. In two dimensions, this medium has a refractive index that decreases from the center line to the edge as the inverse hyperbolic cosine,

$$n(w) = \frac{1}{\cosh(\frac{\mathrm{Re}(w)}{\alpha})}, \tag{3}$$

where the parameter α is the same as that in Eq. (1).

In general, the Mikaelian lens occupies the whole w plane. However, we can employ the fact that in this lens light rays are periodic in the v direction with a period of $D = 2\alpha\pi$ and truncate the lens at $v = \pm D/2$ (see in Fig. 2(a)). When we identify the dashed lines $v = D/2$ and $v = -D/2$

to make a virtual cylinder just as has been described above, light rays will form closed trajectories on this cylinder. The refractive index profile on this cylinder is shown in Fig. 2(b). When a ray enters the upper sheet via the branch cut, it makes a closed loop around the cylinder and leaves the upper sheet through the branch cut in the original direction; this way the upper sheet, and hence the whole device, becomes invisible.

C. The conformal invisible device

As we have shown above, the upper sheet of the virtual space described by Eq. (1) can be folded into a cylinder. We can therefore simply put the truncated Mikaelian lens into the upper sheet to guide light rays (in red) back to the lower sheet through the branch cut (Fig. 1d). In equivalent diagram Fig. 1(e), light ray (in red) has a closed curved trajectory on a cylindrical surface. After mapping to physical space (see in Fig. 1(f)), light ray changes into a curve (in red), which propagates to infinity in the original direction. Light rays that do not touch the branch cut (in purple), do not change their trajectories.

To achieve invisibility, we must carefully choose the parameters α and β in Eq. (1) so that all light rays that meet the branch cut can return to it. First let us fix the parameter α, which means that the width of the upper sheet and the truncated Mikaelian lens will not change. In Fig. 1(d), the length of branch cut will change when β varies. Any light ray starting from any point of the branch cut will return to itself, as long as the length of branch cut is no longer than half the width of the truncated Mikaelian lens, which gives,

$$d \le D/2. \tag{4}$$

Now we have designed a conformal invisible device for all angles. In physical space shown in Fig. 1(f), the refractive index distribution of the designed device is calculated by Eqs. (1)-(3) as

$$n(z)=\begin{cases} \left|1+\dfrac{2\alpha\beta}{z^2-\beta^2}\right| = \dfrac{\sqrt{(x^2-y^2-\beta^2+2\alpha\beta)^2+4x^2y^2}}{\sqrt{x^2+y^2-\beta^2-2x\beta}\sqrt{x^2+y^2-\beta^2+2x\beta}} & \text{inside yellow curve} \\ \dfrac{\left|1+\dfrac{2\alpha\beta}{z^2-\beta^2}\right|}{\cosh\left(\dfrac{\mathrm{Re}(w)}{\alpha}\right)} = \dfrac{2\sqrt{(x^2-y^2-\beta^2+2\alpha\beta)^2+4x^2y^2}}{\exp(x/\alpha)(x^2+y^2+\beta^2-2x\beta)+\exp(-x/\alpha)(x^2+y^2+\beta^2+2x\beta)} & \text{outside yellow curve} \end{cases}. \tag{5}$$

In designing devices using conformal transformation optics, it is necessary to optimize the refractive index distribution so that the values are accessible to experimental fabrication. In our conformal invisible device, the refractive index distribution is determined by α and β. According to Eq. (4), it is easy to show that the maximum value of refactive index distribution in our device is 5.127 when the ratio of α and β equals 3.06384 (see in Appendix). Moreover, we can tune α and β to achieve invisible devices of different sizes.

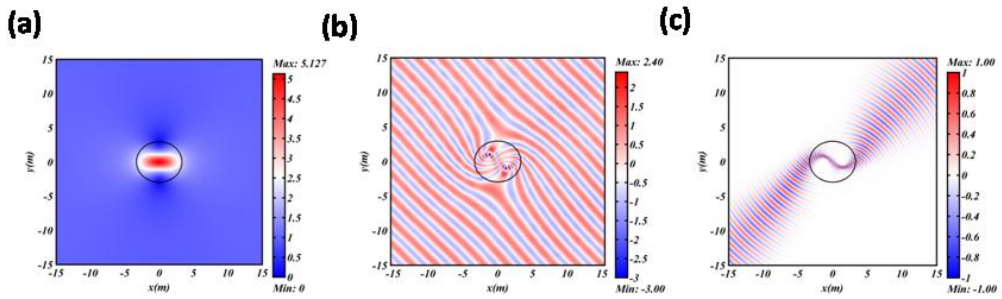

FIG. 3. (a) Refractive index distribution. (b) Field pattern for an incident plane wave. (c) Field pattern for an incident Gaussian beam. The wavelengths of plane wave and Gaussian beam are $\lambda = 8\pi / \sqrt{l(l+1)}$ with $l = 10$ and $l = 20$, respectively.

In Fig. 3a we show the contour of refractive index distribution when α and β equal 4 and 1.30555, respectively. The maximum value is located at the center line. In Fig. 1(f), red trajectories show how our invisible device bends light rays to make itself invisible in geometric optics. In the realm of electromagnetic waves, the phase of the wave must be taken into consideration. In Fig. 1(e), light rays entering into the upper sheet have an extra optical length compared to those that do not touch the branch cut. For a plane wave propagating in virtual space, the wave front will undergo an extra uniform phase shift on the upper sheet, which in general will disturb the plane wave front in the vicinity of the branch cut due to a jump of the phase. However, if this extra uniform phase shift is an integer multiple of 2π, then there is no phase jump and the plane wave will be recovered as it leaves the device. Intrinsically, this phase shift is due to the excitation of a cavity mode in the upper sheet [32,33]. If we think of the truncated Mikaelian lens as a cavity, its eigen wavelength satisfies the relation [29]

$$\lambda = 8\pi / \sqrt{l(l+1)}\,. \qquad (6)$$

In Fig. 3(b) we plot electric field distribution of the invisible device of Fig. 3(a), where $l = 5$. In Fig. 3(c), we use a Gaussian beam to show the function of the designed device. In the previous conformal cloaking design [1,18,19], the impedance is slightly mismatched along the branch cut, which results in some scattering. In our present conformal invisible device, the impedance is unity on both sides of the branch cut. As far as we know, conformal invisible devices with impedance matched everywhere have not been proposed before. In Figs. 3(b) and 3(c) the numerical results show that the invisibility performance of the designed device is almost perfect, without any scattering. The refractive index distribution of this device ranges from 0 to 5.127, which makes the manufacture of such conformal invisible device practical.

D. The conformal invisible cloak

In addition, our device has a capability of making invisible a perfect electrical conductor (PEC). Suppose a linear PEC is inserted along the thick black line segment in physical space shown in Fig. 4(c), light rays entering into the region inside the yellow curve will be reflected by the PEC twice and continue to infinity without changing their direction. In virtual space shown in Fig. 4(a), the PEC is shown as three thick black straight lines, which symmetrically divide the upper sheet into

identical parts. In fact, the two boundary lines of the upper sheet can become one if we roll this sheet into a cylindrical surface. When light rays (in red) enter onto the upper sheet from the branch cut, they propagate along a sine-like curve and are reflected twice by the PEC. Then they return to the lower sheet with their direction and position conserved. The corresponding propagation of light rays is shown in Fig. 4(b). This cloaking device can also work in the realm of electromagnetic waves. In Figs. 4(e) and 4(f), the wavelength is the same as that in Figs. 3(b) and 3(c). For comparison, the scattering field pattern of a PEC without the invisibility device is shown in Fig. 3(d). The simulation results show good performance for cloaking of a PEC.

The ability of our invisibility device to hide a linear PEC can be employed for turning it into a regular invisibility cloak. To do this, we can use an additional geometric transformation, either the Zhukowski mapping or the transformation used in carpet cloaks [5,6], to expand the PEC and create an invisible region. Importantly, there is fundamental difference between the resulting invisible cloak and the carpet cloaks. In particular, the present cloak will work for light coming from any direction while the carpet cloak is really invisible only for light coming from one direction.

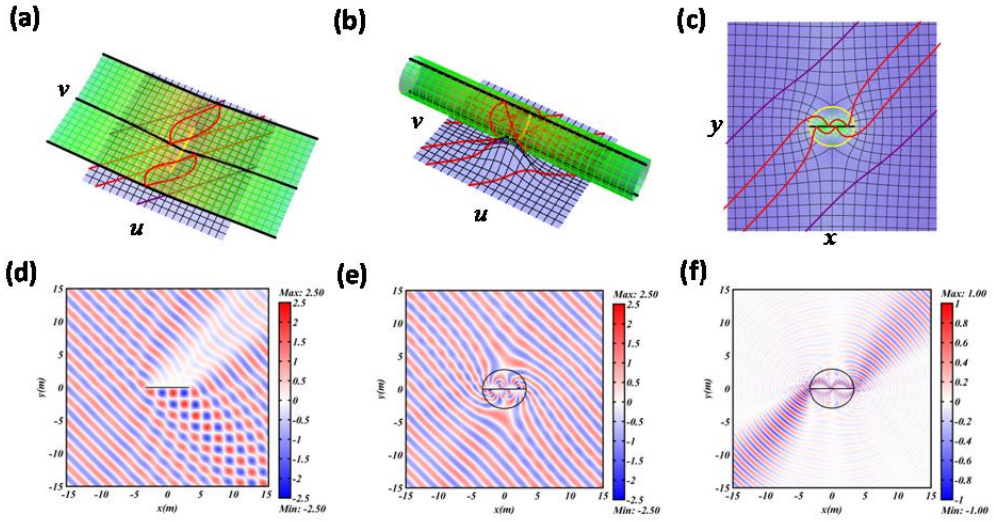

FIG. 4. (a) Virtual space of cloaking a PEC. (b) The equivalent diagram of virtual space of cloaking a PEC. (c) Physical space of cloaking a PEC. (d) The scattering field pattern of a PEC in air for an incident plane wave. (e) The field pattern of a PEC inside our invisible device for an incident plane wave and (f) for an incident Gaussian beam. The wavelengths of plane wave and Gaussian beam are $\lambda = 8\pi / \sqrt{l(l+1)}$ with $l = 10$ and $l = 20$, respectively.

III.Conclusion

We have designed a conformal invisible device via conformal transformation optics, which only

needs an isotropic refractive index distribution. By tuning the parameters of conformal mapping and using a truncated Mikaelian lens with a suitable width, we dramatically deduce the maximum value of refractive index distribution to 5.127, which makes the device accessible to experimental fabrication. In virtual space, the refractive index is 1 on both sides of the branch cut, which means that the impedance is fully matched at the branch cut. So the invisibility is perfect: there is no scattering. Our design can also hide a linear PEC within it, and even a PEC object if a further coordinate transformation is applied. As far as we know, H-fractal metamaterials can be used to achieve refractive indexes from 0 to 1 for microwave frequencies [34]. In addition, by drilling holes on high dielectrics or using H shape metamaterials, one can obtain refractive indexes larger than 1 [35]. With these methods, we hope that our work will stimulate a proof-of-principle experiment.

Acknowledgements

This work was supported by the National Science Foundation of China for Excellent Young Scientists (Grant No. 61322504), the Foundation for the Author of National Excellent Doctoral Dissertation of China (Grant No. 201217), and the Priority Academic Program Development (PAPD) of Jiangsu Higher Education Institutions. T. T. was supported by the grant P201/12/G028 of the Czech Science Foundation. S. A. C. and Y. X. were supported by a Multidisciplinary University Research Initiative from the Office of Naval Research (Grant No. N00014-13-1-0631).

References

[1] U. Leonhardt, *Optical conformal mapping*, Science **312**, 1777 (2006).

[2] J. B. Pendry, D. Schurig, & D. R. Smith, *Controlling Electromagnetic Fields,* Science **312**, 1780 (2006).

[3] D. Schurig, J. J. Mock, B. J. Justice, S. A. Cummer, J. B. Pendry, A. F. Starr, & D. R. Smith, *Metamaterial electromagnetic cloak at microwave frequencies*, Science **314**, 977(2006).

[4] U. Leonhardt, & T. Tyc, *Broadband Invisibility by Non-Euclidean Cloaking*, Science **323**, 100 (2009).

[5] J. Li, & J. B. Pendry, *Hiding under the Carpet: A New Strategy for Cloaking*, Phys. Rev. Lett. **101**, 203901 (2008).

[6] R. Liu, C. ji, J. J. Mock, J. Y. Chin, T. J. Cui & D. R. Smith, *Broadband ground-plane cloak*, Science **323**, 366 (2009).

[7] M. Rahm, D. Schurig, D. A. Roberts, S. A. Cummer, D. R. Smith, & J. B. Pendry, *Design of electromagnetic cloaks and concentrators using form-invariant coordinate transformations of Maxwell's equations*, Photon. Nanostr. **6**, 87 (2008).

[8] M. M. Sadeghi, S. Li, L. Xu, B. Hou, & H. Y. Chen, *Transformation optics with Fabry-Pérot resonances*, Sci. Rep. **5**, 8680 (2015).

[9] H. Y. Chen, & C. T. Chan, *Transformation media that rotate electromagnetic fields*, Appl. Phys.Lett. **90**, 241105 (2007).

[10] H. Y. Chen, B. Hou, S. Chen, X. Ao, W. Wen, & C. T. Chan, *Design and Experimental Realization*

of a Broadband Transformation Media Field Rotator at Microwave Frequencies, Phys. Rev. Lett. **102**, 183903 (2009).

[11] H. Y. Chen, C. T. Chan, & P. Sheng, *Transformation optics and metamaterials*, Nat. Meterials **9**, 387 (2010).

[12] A. V. Kildishev, & V. M. Shalaev, *Transformation optics and metamaterials*, Phys.-Usp. **54**, 53 (2011).

[13] Y. Liu, & X. Zhang, *Recent advances in transformation optics*, Nanoscale **4**, 5277 (2012).

[14] B. Zhang, *Electrodynamics of transformation- based invisibility cloaking*, Light: Science & Applications **1**, e32 (2012).

[15] H. Y. Chen, & C. T. Chan, *Acoustic cloaking in three dimensions using acoustic metamaterials*, Appl. Phys. Lett. **91,** 183518 (2007).

[16] M. T. Michael, *A fundamental Lagrangian approach to transformation acoustics and spherical spacetime cloaking*, Europhys. Lett. **98,** 34002 (2012).

[17] C. García-Meca, S. Carloni, C. Barceló, G. Jannes, J. Sánchez-Dehesa, & A. Martínez, *Analogue Transformations in Physics and their Application to Acoustics*, Sci. Rep. **3,** 2009 (2013).

[18] L. Xu, & H. Y. Chen, *Conformal transformation optics*, Nat. Photonics **9,** 16 (2015).

[19] Q. Wu, Y. Xu, H. Li, & H. Y. Chen, *Cloaking and imaging at the same time*, Europhys. Lett. **101,** 34004 (2013).

[20] L. Xu, & H. Y. Chen, *Logarithm conformal mapping brings the cloaking effect*. Sci. Rep. **4,** 6862 (2014).

[21] K. Yao, & X. Jiang, *Designing feasible optical devices via conformal mapping*, J. Opt. Soc. Am. B **28,** 1037 (2011).

[22] X. Jiang, K. Yao, Q. Wu, Y. Xu, & H. Y. Chen, *Conformal transformations to achieve unidirectional behavior of ligh,* New J. Phys. **14,** 053023 (2012).

[23] H. Y. Chen, Y. Xu, H. Li, & T. Tyc, *Playing the tricks of numbers of light sources*, New J. Phys. **15,** 093034 (2013).

[24] C. Gu, K. Yao, W. Lu, Y. Lai, H. Y. Chen, B. Hou, & X. Jiang,*Experimental realization of a broadband conformal mapping lens for directional emission*, Appl. Phys. Lett. **100,** 261907 (2012)

[25] Y. Ma, Y. Liu, L. Lan, T. Wu, W. Jiang, C. K. Ong, & S. He, *First experimental demonstration of an isotropic electromagnetic cloak with strict conformal mapping*, Sci. Rep. **3,** 2182 (2013).

[26] A. J. Henn, & U. Leonhardt, *Ambiguities in the Scattering Tomography for Central potentials*, Phys. Rev. Lett. **97**, 073902 (2006).

[27] T. Tyc, H. Y. Chen, A. Danner, & Y. Xu, *Invisible lenses with positive isotropic refractive index,* Phys. Rev. A **90**, 053829 (2014).

[28] A.L. Mikaelian, The use of medium properties to focus waves, Doklady of the USSR Academy of Sciences, Issue 81, pp. 569-571 (1951).

[29] A. L. Mikaelian & A. M. Prokhorov, *Self-focusing media with variable index of refraction*, Prog. Opt. **17,** 283 (1980).

[30] Z. Nehari, *Conformal Mapping,* (McGraw-Hill, New York, 1952).

[31] U. Leonhardt, & T. Philbin, *Geometry and light: the science of invisibility*, (Dover, 2010).

[32] H. Y. Chen, U. Leonhardt, & T. Tyc, *Conformal cloak for waves*, Phys. Rev. A **83,** 055801 (2011).

[33] H. Li, Y. Xu, & H. Y. Chen, *Conformal cloaks at eigenfrequencies*, J. Phys. D: Appl. Phys. **46,** 135109 (2013).

[34] Q. Wu, X. Feng, R. Chen, C. Gu, S. Li, H. Li, Y. Xu, Y. Lai, B. Hou, H. Y. Chen, & Y. Li, An inside-out Eaton lens made of H-fractal metamaterials. Appl. Phys. Lett. **101,** 031903 (2012).

[35] C. Gu, K. Yao, W. Lu, Y. Lai, H. Y. Chen, B. Hou, & X. Jiang, Experimental realization of a broadband conformal mapping lens for directional emission, Appl. Phys. Lett. **100,** 261907 (2012).

APPENDIX: THE MAXIMUM VALUE OF REFRACTIVE INDEX DISTRIBUTION IN CONFORMAL INVISIBLE DEVICE

In this appendix, we give a mathematical derivation of the maximum value of refactive index distribution in conformal invisible device.

As mentioned in the main text, to achieve invisible property, the length of branch cut in virtual space should not be longer than half of width of the truncated Mikaelian lens, which gives Eq. (4). We will use this condition to obtain the maximum value of refractive index distribution.

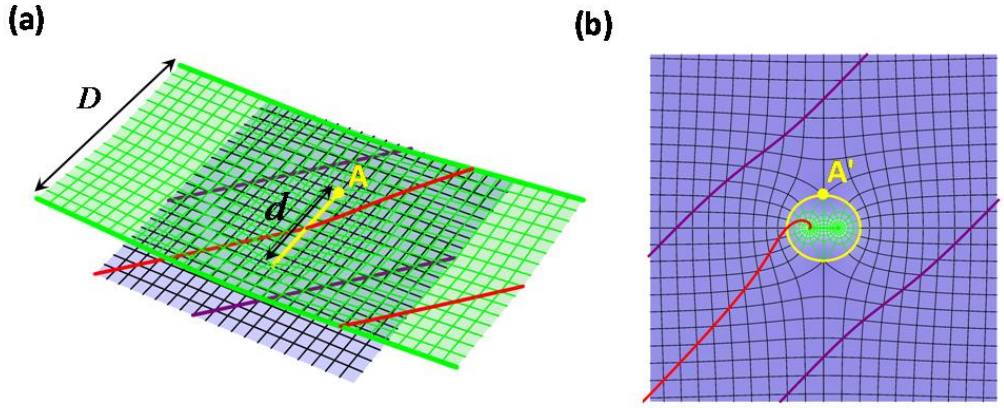

FIG. 5. (a) Virtual space of conformal logarithmic mapping. (b) Physical space of conformal logarithmic mapping.

The details of conformal logarithmic mapping (Eq. (1)) is shown again in Fig. 5. Let A ($u_0 + v_0 i$) and A' ($x_0 + y_0 i$) be two corresponding points in virtual space and physical space of conformal mapping. In Fig. 5(a), the width of the upper sheet is $D = 2\alpha\pi$, while the length of branch cut (in yellow) is d . Eq. (4) implies that

$$\mathrm{Re}\left(x_0 + y_0 i + \alpha \log\left(x_0 - \beta + y_0 i\right) - \alpha \log\left(x_0 + \beta + y_0 i\right)\right) = 0 , \tag{7}$$

and

$$\mathrm{Im}\left(x_0 + y_0 i + \alpha \log\left(x_0 - \beta + y_0 i\right) - \alpha \log\left(x_0 + \beta + y_0 i\right)\right) \le \frac{\alpha\pi}{2} . \tag{8}$$

Eq. (7) can be re-expressed as

$$
\begin{aligned}
&\mathrm{Re}\left(x_0 + y_0 i + \alpha \log\left(x_0 - \beta + y_0 i\right) - \alpha \log\left(x_0 + \beta + y_0 i\right)\right) \\
&= \mathrm{Re}\left(x_0 + y_0 i + \alpha \log\left(\frac{\sqrt{x_0^2 + y_0^2 + \beta^2 - 2x_0\beta}\exp\left(i\left(\arctan\left(\frac{y_0}{x_0 - \beta}\right)\right)\right)}{\sqrt{x_0^2 + y_0^2 + \beta^2 + 2x_0\beta}\exp\left(i\left(\arctan\left(\frac{y_0}{x_0 + \beta}\right)\right)\right)} \right) \right), \\
&= x_0 + \frac{\alpha}{2}\log\left(\frac{x_0^2 + y_0^2 + \beta^2 - 2x_0\beta}{x_0^2 + y_0^2 + \beta^2 + 2x_0\beta}\right) \\
&= 0
\end{aligned}
$$

which means

$$
1 - \frac{4x_0\beta}{x_0^2 + y_0^2 + \beta^2 + 2x_0\beta} = \exp\left(-\frac{2x_0}{\alpha}\right).
$$

When $x_0 \to 0$, we obtain

$$
1 - \frac{4x_0\beta}{x_0^2 + y_0^2 + \beta^2 + 2x_0\beta} \to 1 - \frac{2x_0}{\alpha},
$$

Therefore with Eq. (7), we have

$$
2\alpha\beta = y_0^2 + \beta^2. \tag{9}
$$

Eq. (8) can be re-expressed as

$$
\begin{aligned}
&\mathrm{Im}\left(x_0 + y_0 i + \alpha \log\left(x_0 - \beta + y_0 i\right) - \alpha \log\left(x_0 + \beta + y_0 i\right)\right) \\
&= \mathrm{Im}\left(x_0 + y_0 i + \alpha \log\left(\frac{\sqrt{x_0^2 + y_0^2 + \beta^2 - 2x_0\beta}\exp\left(i\left(\arctan\left(\frac{y_0}{x_0 - \beta}\right)\right)\right)}{\sqrt{x_0^2 + y_0^2 + \beta^2 + 2x_0\beta}\exp\left(i\left(\arctan\left(\frac{y_0}{x_0 + \beta}\right)\right)\right)} \right) \right). \\
&= y_0 + \alpha\left(\pi + \arctan\left(\frac{y_0}{x_0 - \beta}\right) - \arctan\left(\frac{y_0}{x_0 + \beta}\right)\right) \\
&\le \frac{\alpha\pi}{2}
\end{aligned}
$$

When $x_0 \to 0$, we obtain,

$$
y_0 + \alpha\left(\pi - 2\arctan\left(\frac{y_0}{\beta}\right)\right) \le \frac{\alpha\pi}{2}. \tag{10}
$$

By combining Eqs. (9) and (10), we can eliminate the variable y_0 and obtain a transcendental inequation,

$$
\sqrt{2(\alpha/\beta)^{-1} - (\alpha/\beta)^{-2}} + \frac{\pi}{2} \le 2\arctan\left(\sqrt{2\alpha/\beta - 1}\right). \tag{11}
$$

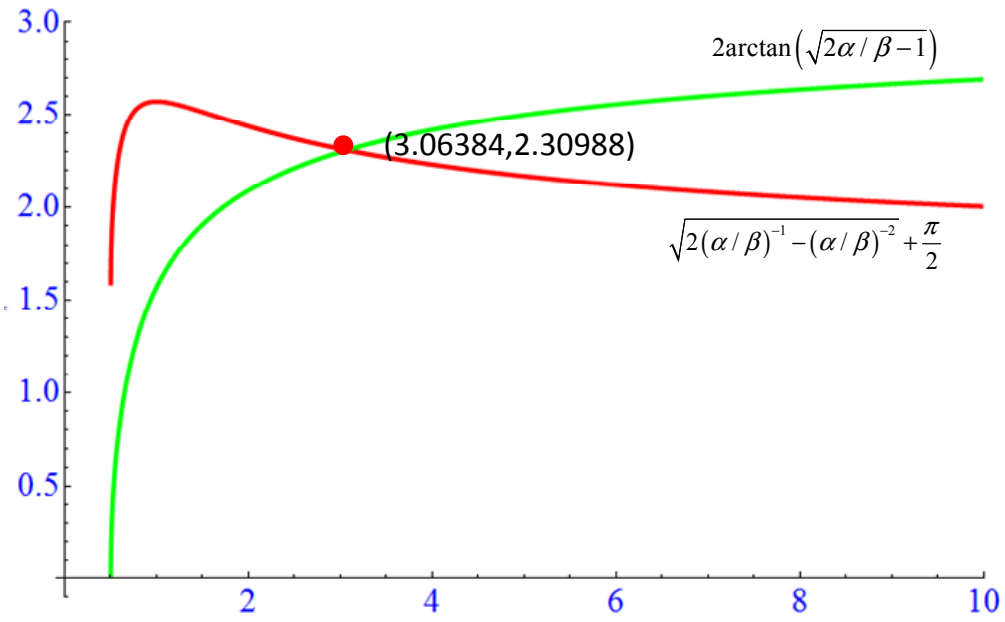

FIG. 6. The solution of the transcendental inequation (11).

We plot graphs of functions on both sides of Eq. (11) in Fig. 6, where the x-axis presents variables α/β. The numerical solution of Eq. (11) is $\alpha/\beta \geq 3.06384$. The minimum value of $n(z)$ in Eq. (5) is then 5.127, which corresponds to of physical space. It is worth to mention that the maximum value of refractive index distribution in conformal invisible device only depends on the ratio of α and β, while α determinates the size of the designed device.